Naval Environmental Prediction Research Facility
Monterey, CA 93943-5006
Contractor Report CR 89-11 July 1989

(4)

INVESTIGATION OF NORTH ATLANTIC FOG AND DEVELOPMENT OF A MARINE FOG FORECAST SYSTEM

C. William Rogers
Calspan Corporation
Buffalo, NY 14225

APPROVED FOR PUBLIC RELEASE, DISTRIBUTION IS UNLIMITED

UNCLASSIFIED

SECURITY CLASSIFICATION OF THIS PAGE

REPORT DOCUMENTATION PAGE

1a. REPORT SECURITY CLASSIFICATION UNCLASSIFIED	1b. RESTRICTIVE MARKINGS
2a. SECURITY CLASSIFICATION AUTHORITY	3. DISTRIBUTION/AVAILABILITY OF REPORT Approved for public release; distribution is unlimited
2b. DECLASSIFICATION / DOWNGRADING SCHEDULE	
4. PERFORMING ORGANIZATION REPORT NUMBER(S) 7589-1	5. MONITORING ORGANIZATION REPORT NUMBER(S) CR 89-11
6a. NAME OF PERFORMING ORGANIZATION Calspan Corporation 6b. OFFICE SYMBOL (If applicable)	7a. NAME OF MONITORING ORGANIZATION Naval Environmental Prediction Research Facility
6c. ADDRESS (City, State, and ZIP Code) P.O. Box 400 Buffalo, NY 14225	7b. ADDRESS (City, State, and ZIP Code) Monterey, CA 93943-5006
8a. NAME OF FUNDING/SPONSORING ORGANIZATION Naval Ocean Systems Center 8b. OFFICE SYMBOL (If applicable) Code 54	9. PROCUREMENT INSTRUMENT IDENTIFICATION NUMBER Contract No. N00014-87-C-0232
8c. ADDRESS (City, State, and ZIP Code) San Diego, CA 92152-5000	10. SOURCE OF FUNDING NUMBERS

10. SOURCE OF FUNDING NUMBERS

PROGRAM ELEMENT NO.	PROJECT NO	TASK NO.	WORK UNIT ACCESSION NO.
62435N	RM35G80	3	DN656766

11. TITLE (Include Security Classification)
Investigation of North Atlantic Fog and Development of a Marine Fog Forecast System (U)

12. PERSONAL AUTHOR(S)
Rogers, C. William

13a. TYPE OF REPORT	13b. TIME COVERED	14. DATE OF REPORT (Year, Month, Day)	15. PAGE COUNT
Final	FROM 6/87 TO 6/89	April 1989	59

16. SUPPLEMENTARY NOTATION

17. COSATI CODES

FIELD	GROUP	SUB-GROUP
04	02	

18. SUBJECT TERMS (Continue on reverse if necessary and identify by block number)
Fog Forecasting System, North Atlantic, TESS (3), Marine Haze, Inversions, Taylor Fog, Stratus Lowering Fog, Visibility

19. ABSTRACT (Continue on reverse if necessary and identify by block number)

A two-year, two-task research effort to study ocean fog and haze, and to provide additional expertise for An Expert-system for Shipboard Obscuration Prediction (AESOP) was carried out. Year 1 (Task 1) studied fog occurrence in the North Atlantic and developed an AESOP rule base for these fogs, which was published in a Program Performance Specification (Rogers, 1988). The Year 2 (Task II) effort evaluated forecast errors generated during a test of AESOP, and modified and extended the rule base to correct for these errors. Additionally, fog dissipation and haze formation and dissipation were examined for the N. Atlantic.

Fog is primarily a summertime phenomenon in the N. Atlantic. The well-known Taylor fog forms at midlatitudes (40-50N) in the stable, relatively shallow marine boundary layer which is located at the western end of the semi-permanent anticyclone. In the eastern

20. DISTRIBUTION/AVAILABILITY OF ABSTRACT ☒ UNCLASSIFIED/UNLIMITED ☐ SAME AS RPT. ☐ DTIC USERS	21. ABSTRACT SECURITY CLASSIFICATION UNCLASSIFIED
22a. NAME OF RESPONSIBLE INDIVIDUAL Dr. Paul M. Tag, contract monitor	22b. TELEPHONE (Include Area Code) (408) 647-4737 22c. OFFICE SYMBOL NEPRF WU 6.2-31BG

DD FORM 1473, 84 MAR 83 APR edition may be used until exhausted. All other editions are obsolete.

SECURITY CLASSIFICATION OF THIS PAGE

UNCLASSIFIED

19. Abstract (Continued)

N. Atlantic extratropical anticyclogenesis occasionally occurs, which can produce stratus lowering fog along its eastern side and Taylor fog in the southerly flow at its western end. At higher latitudes (50-60N) in the track of the transient synoptic systems, much of the fog is advected in from the Taylor-fog formation regions to the south and west.

Fog dissipation is driven primarily by heating produced by absorption of solar radiation and mixing of warm air from above the inversion which caps the fog layer. These two dissipation processes are abetted by the mixing of the lower humidity of the warm air.

Over the open ocean, the aerosol concentration is generally too low to provide even the minimum concentration required to produce a maximum haze visibility of 5 n mi (9.25 km). Haze visibility levels, without the presence of drizzle or rain, are found over the open ocean mainly in regions of fog formation and dissipation.

CONTENTS

1. INTRODUCTION

Under contract No. N00014-87-C-0232 with the Naval Environmental Prediction Research Facility, Calspan Corp. engaged in a two-year, two-task research effort to study ocean fog and haze and to provide additional expertise for An Expert-system for Shipboard Obscuration Prediction (AESOP). Year 1 (Task I) involved a study of fog occurrence in the North Atlantic and development of an AESOP rule base for these fogs, which was published in a Program Performance Specification (PPS) (Rogers, 1988). The Year 2 (Task II) effort focused first on evaluation of forecast errors generated during a test of AESOP, and modification of and additions to the rule base to correct these errors. Secondly, we examined fog dissipation as well as haze formation and dissipation with the goal of providing rules to AESOP for these occurrences. This report describes the data sets, data analyses and results of the two-year research effort.

In 1981, Rogers et al. prepared a fog forecasting approach for the west coast of the United States. This procedure took the form of a decision tree which considered the parameters and physical processes important to the formation of stratus lowering fog, the primary fog type along the west coast. Based on this work and the results of three on-shore and eight maritime field programs conducted during the 1970's, Martin Marietta Data Systems undertook in 1987 the development for the Navy of an expert system for fog forecasting and dubbed it AESOP. Because the Navy's interests lie considerably beyond and outside the west coast region, a study of fog occurrence in the N. Atlantic was

initiated, with the goal of developing a fog forecasting approach for the predominant fog type there, i.e. Taylor fog--named after G. I. Taylor who first discussed these fogs (Taylor, 1917). The resulting decision tree was published in the form of a program performance specification (Rogers, 1988). This decision tree was added to the earlier procedure for west coast fog, to produce the rule base for the AESOP version whose test run we evaluated at the beginning of Task II. Throughout Task II we provided the AESOP developer with modifications and improvements to the rule base as our research effort warranted.

Section 2 of this report provides a summary of fog and haze formation and dissipation processes over the N. Atlantic ocean as determined from this study, previous field study cruises and theoretical investigations. Section 3 describes the selection of the fog data set for the N. Atlantic and presents in tabular form the fog observations, inversion types and synoptic situations from which the fog forecast rules were developed for AESOP in Task I. Section 4 presents the application of fog formation and dissipation processes to fog forecasting, while Section 5 provides the same information for haze formation and dissipation. Section 6 describes the analyses of the AESOP forecast failures generated during the test of AESOP on the North Atlantic data set.

2. SUMMARY OF FORMATION AND DISSIPATION PROCESSES OF ATLANTIC FOG AND HAZE

2.1 Fog Formation and Dissipation

Fog over the unfrozen N. Atlantic is primarily a summertime phenomenon when relatively shallow or stable marine boundary layers (MBL's) frequently occur. In winter the region is dominated by vigorous cyclonic activity. In the southerly flow to the east of these cyclones, upward vertical motion distributes throughout a deep layer any cooling produced at the surface. On the other hand, in the northerly flow to the west of these cyclones where downward motion works to produce inversion-capped MBL's, the strong heating of the air by the underlying ocean works to deepen the boundary layer (BL). Thus, the shallow MBL's and their associated fogs are very rare during the winter.

The summertime circulation in the N. Atlantic is dominated by the semi-permanent, subtropical anticyclone in the south and transient, weak cyclones and troughs moving eastward along the northern edge of the anticyclone. The western end of the anticyclone is the location of southerly flow of warm moist air which is continually cooled as it flows northward over progressively colder water. This condition works to produce a stable, relatively shallow MBL which is the home of the well known Taylor fog.

Eastward from the midpoint of the transient systems' track, extratropical anticyclogenesis occasionally occurs, which produces along its eastern side a relatively shallow MBL capped by a stratus deck, and thus the conditions for stratus lowering fog. The southerly flow at the western end of these highs is a

site for Taylor fog, albeit the sea surface temperature (SST) gradient is weaker than that found further west.

At the relatively high latitudes (50-60N) of this track of transient systems, much of the fog is advected in from the Taylor fog formation regions to the south and west. In such southerly flow ahead of lows and troughs, upward vertical motion deepens the BL in which the Taylor fog formed and fog can occur at the base of this well-mixed, somewhat deeper MBL.

In addition, slowly moving cut-off low pressure systems occur in this transient system track. Fog forms near the center of these lows, which are characterized by a moderately deep, nearly saturated MBL with low surface wind speeds. The formation process is probably related to the production of a shallow surface layer with an inverted temperature profile, from cooling by small scale pools of slightly colder ocean water.

Fog dissipation can be driven by 1) heating of the fog, 2) mixing in of unsaturated air or 3) upward vertical motion which increases the depth of the MBL and lifts the fog away from the ocean surface. Of these processes, heating occurs in three ways: sensible heat flux from the ocean surface, absorption of solar radiation by the fog drops, and mixing of warmer air into the foggy MBL. The last process usually takes place simultaneously with the mixing of unsaturated air.

Although in theory these processes can all work in conjunction, in actuality the atmospheric flow patterns present in the N. Atlantic in summer prevent this from happening. For example, the raising of the inversion height and deepening

of he BL occur ahead of migratory short waves where the surface flow is southerly. This flow experiences cooling as it moves northward over the progressively colder ocean water. In addition, middle and upper clouds are usually present ahead of the upper level trough so that solar radiation near the surface is greatly reduced. Similarly, because the SST isotherms lie generally east-west, air flow with a northerly component is required for air to be heated by the ocean. Such surface flow is located to the rear of cold fronts and troughs, while the fog, usually of the Taylor-type, occurs in the southerly flow ahead of these features.

One situation where many fog dissipation processes do work in concert is stratus-lowering fog, occurring at the eastern end of an anticyclone. Here 1) the northeasterly flow moves over warmer water, 2) solar insolation can penetrate to the low levels because of the absence of middle and high clouds, and 3) warmer, unsaturated air can be mixed through the subsidence inversion which caps the MBL.

The AESOP rule base evaluates the various combinations of dissipation factors as a function of observed and forecast conditions and arrives at the likelihood of fog dissipation.

2.2 Haze Formation and Dissipation

Haze, for this study of forecasting obscuration over the ocean, is defined as visibility greater than one n mi and less than or equal to five n mi. The lower limit is imposed by the visibility definition for fog (visibility less than or equal to one n mi); the upper limit arises from the resolution of

visibility levels reported in the ocean ship surface weather code, i.e., 2, 5, and 10 n mi., with the last being too large for haze.

Haze is usually thought of as occurring when relative humidity reaches high values and aerosols deliquesce and grow to sizes where they can effectively scatter visible light. However, a minimum number of particles per unit volume is required to scatter enough light to reduce visibility to a haze value of 5 n mi. Observations from two transatlantic cruises (Mack et al., 1978 and Hoppel et al., 1988) indicate that over the open ocean the aerosol concentration is generally too low to provide even the minimum concentration required to produce the maximum haze visibility. Thus it appears that reduction of visibilities to haze levels with increasing relative humidity over the open ocean is a relatively rare occurrence. However, this process does occur in coastal areas where the number of nuclei is made sufficiently large by the proximity of land sources. These nuclei can be both natural and anthropogenic (Mack and Niziol, 1978; Mack et al., 1977; Wattle, 1987; Mack et al., 1983; and Hoppel et al., 1988).

Haze visibility levels, without the presence of drizzle or rain, are found over the open ocean mainly in regions of fog formation and dissipation. However, since observations indicate that this condition is both transient in time and small scale in space, so that it is a relatively rare event, haze formation and dissipation should be treated in AESOP primarily in the context of fog life cycles.

3. NORTH ATLANTIC FOG DATA SET AND SELECTED YEAR1 RESULTS

3.1 Case Selection

Case selection began with NEPRF processing the FNOC archival tapes of surface ship reports in the N. Atlantic. This data base begins in November 1970. In addition to surface reports, vertical soundings were required since the temperature profile is a crucial piece of information about fog formation. Therefore, the useful raw data base was limited to the time period during which weather ships operated and produced radiosondes. A list of the N. Atlantic weather ships and their approximate locations is given in Table 1.

Table 1. Approximate Locations of N. Atlantic Weather Ships

SHIP	LATITUDE	LONGITUDE
4YA	62N	33W
4YB	56N	51W
4YC	53N	35W
4YD	45N	41W
4YE	35N	48W
4YH	38N	72W
4YI	59N	19W
4YJ	53N	19W
4YK	45N	16W
4YM	66N	2E

Since the the weather ship program was discontinued in 1977, the raw data base extended from November 1970 to December 1976. Case selection was restricted to the winter (December through February) and summer (June through August) seasons.

The 1200 GMT surface ship reports were examined for fog occurrence; the number of ship reports is a maximum at this radiosonde observation time. If fog occurred at 1200 GMT,

then the 1800 GMT report was examined for fog occurrence. Two categories of fog occurrence were established, fog at both times and fog only at 1200 GMT. The purpose of this discrimination was to enhance selection of fogs which were dense, continuous and long lasting (i.e., having withstood solar insolation), as opposed to those which were tenuous, patchy and short-lived. Both types of fog occurrence formed the initial data base.

The results of the NEPRF processing of the raw data set included daily maps which showed the locations of the ship reports that had satisified the fog occurrence criteria. Distinction was made between the two types of fog occurrence by using different plot symbols. Further distinction was made by plotting the results for the weather ships as two additional symbols. These maps were then delivered to Calspan for further case selection.

Because of the requirement for vertical profiles of temperature, the cases were limited to fog occurences at and around the weather ship locations. In order to concentrate our study on wide areas of fog rather than small fog patches, we attempted to utilize only those fogs for which at least four transient ships reported fog within a ten degree, latitude-longitude box centered at the weather ship. Furthermore, we concentrated our selection on those instances in which the weather ship reported fog at both 1200 and 1800 GMT. In practice, this procedure worked well for the summer; but it proved entirely too restrictive for the winter season because of the scarcity of transient ships. As a result,

fog occurrence at weather ships alone was used to select winter cases.

From the ship report tapes, fog occurrence was defined using both the observation of present weather and the visibility. The surface ship synoptic code allows for 100 different kinds of present weather, with each decade assigned to major occurrences of a particular weather phenomenon, e.g., 40's for fog, 50's for drizzle and 60's for rain. Obviously, the fog data set included the present weather reports of fog (codes 40 through 49) and 28 (for fog occurring in the past hour) regardless of visibility. In addition, the other present weather reports of fog (codes 10, 11 and 12) were included if the visibility was less than or equal to 1 n mi.

3.2 Winter Cases

The six winter seasons covering December 1970 to February 1976 produced only eight cases of true fog, and only three of these reported visibility less than or equal to 1/4 n mi. Obviously, fog is a rare event in the N. Atlantic during the winter. This result is to be expected since the N. Atlantic in the winter is dominated by cyclonic activity with its associated strong winds and copious precipitation, both of which are detrimental to fog formation.

A number of the winter fogs occurred with southerly wind on the west side of a high pressure system which had managed to forge northward into the region north of 45N, usually dominated by cyclonic activity. The formation of these fogs is not unlike

that of the Taylor fogs encountered during the summer, with flow of warm moist air over increasingly colder water.

3.3 Summer Cases

Our study investigated 68 cases of summer fog in the N. Atlantic; 62 were the Taylor-type fog and six were the stratus lowering-type fog. The Taylor-type fog predominated in the western Atlantic where the surface air flow is predominantly from warmer to colder water and the SST gradients are climatologically larger than in the eastern Atlantic. Both Taylor-type and stratus lowering fogs occur in the eastern Atlantic where both northeasterly flow with stratus and southerly flow across the weaker SST gradient occur around the anticyclones which develop in the eastern N. Atlantic.

It cannot be emphasized enough that fog in the N. Atlantic is intimately related to the synoptic weather pattern. These patterns control not only the flow of moist air over colder water but they produce the vertical motion that is critically important to fog formation. It is the vertical motion which controls the depth and thermal stability of the MBL, and thus the formation, persistence and dissipation of fog. In many cases the forecaster does not have explicit information on these BL parameters. The forecast procedure developed in Year 1 (Roger ., 1988) utilizes synoptic data to provide implicit information about the BL. Several important examples are illustrative:

Fog occurs mostly with southerly winds (i.e., 100 through 260 degrees), which during the summer occur on the west side of anticyclonic systems. In the case of quasi-steady state,

semi-permanent highs, this region has little vertical motion. The observed surface-based, inverted temperature profiles are then produced by the strong cooling from the cold ocean water. In the case of anticyclogenesis, subsidence and its associated low level inversions occur on the west side of the high. These inversions, coupled with southerly flow, act together to form strong surface-based, inverted temperature profiles.

In the eastern N. Atlantic, fog occurs predominantly with raised inversions capping an MBL in which the temperature is lapsed. At the latitudes north of 55N (4YI) the SST gradient is relatively weak and the area is characterized by the passage of low pressure troughs. Thus, fog at these latitudes in the eastern Atlantic is primarily the result of fog formed further south by cooling over colder water; this fog then moves northward in the upward vertical motion ahead of a trough, producing a marine layer capped by an inversion.

At lower latitudes (53N, 4YJ), fog occurs with both surface-based inversions and raised inversions above a lapsed MBL. The surface inversions occur with the combination of southerly flow over colder water and the subsidence on the west side of high pressure area, as indicated above.

The raised inversion fogs are of two types; one is similar to those that occur further north both in the eastern and western Atlantic. The second type occurs with northeasterly winds from colder to warmer water, with the surface air temperature colder than the water. These fogs may be either stratus lowering fogs or initial fogs that are slowly being heated by the ocean

surface.

In the fog forecast procedure developed under Task I, various types of vertical temperature profiles are used. These profiles are illustrated in Fig. 1 and described below:

Type 1--A surface-based inversion exists with a moderate to strong increase in temperature in the vertical; a maximum temperature is reached within the 100 to 200m layer.

Type 2--A weak surface-based inversion with a strength of 0.5 C per 200 m extends to approximately 200m; this inversion is generally capped by a stronger inversion.

Type 3--A lapsed MBL is capped by an inversion whose height and strength depend on the sign and strength of the associated vertical motion.

Much of the PPS prepared under Task 1 (Rogers, 1988) was devoted to the details of estimating these profiles and their height from synoptic flow patterns.

3.4 N. Atlantic Inversion Types, Fog Types and Synoptic Situations

Much of the analysis performed during Task I involved determination of the MBL structure from the radiosonde observations. Inversion height and strength were determined for each case, and the characteristic inversion types shown in Fig. 1 were defined by categorization of the complete set. The surface synoptic charts and the inversion characteristics were analyzed for each case to determine the fog type: stratus lowering (ST), Taylor formation (TF), Taylor advection (TAD), Taylor deepening (TDP) and center of low (COL). The subsets of these data for each characteristic inversion type were then analyzed to

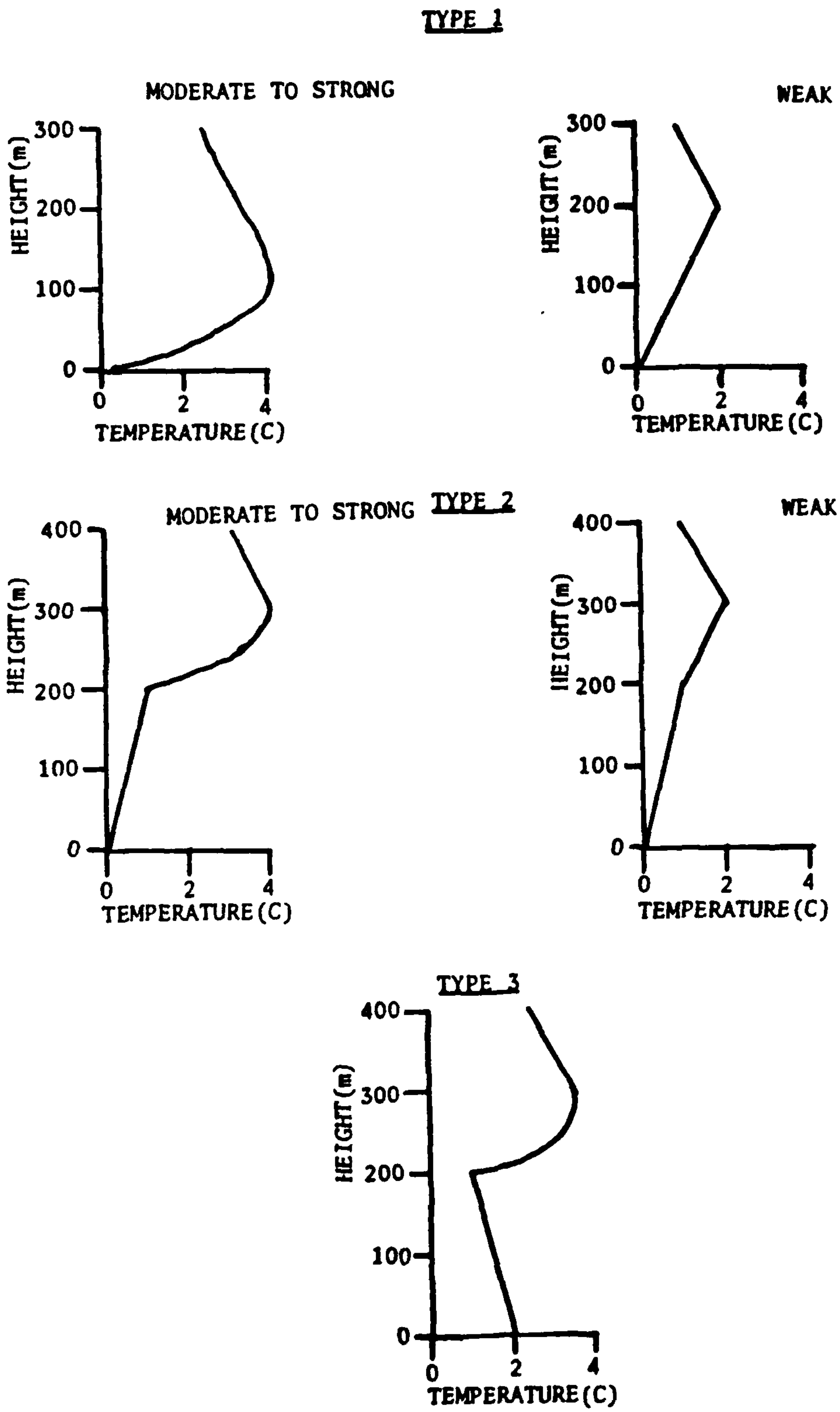

Figure 1. Illustration of inversion types associated with N. Atlantic fog.

provide the correlations between fog type, inversion type and synoptic situation.

The basic data set as defined from the present weather code and the visibility levels was discussed in Section 3.1. For our analysis, NEPRF provided us with all 0000 and 1200 GMT observations for the 48 hour period centered on the 1200 GMT fog case time. Examination of these data showed numerous observations of visibility less than or equal to one n mi with present weather of intermittent or continuous slight drizzle. The rules for reporting surface present weather require that, in the case of two phenomena occurring simultaneously, the one that has the higher code number is reported. Thus, fog could be present in those cases where drizzle was reported. On the other hand, drizzle alone can produce visibility restrictions at and below one n mi.

By reference to Calspan's numerous observations of visibility in drizzle at sea, we developed the following criterion to specify simultaneous occurrence of fog and drizzle. Drizzle can reduce the visibility to no lower than one-half n mi. Therefore, any present weather observations of drizzle in which the visibility was reported at or below 1/4 n mi were classified as also having fog. This convention was followed in the definition of cases for the fog study. Table 2 defines the present weather code as used in the case summaries.

Table 2. Selected WMO Present Weather Codes and Descriptions

CODE FIGURE	DESCRIPTION OF PRESENT WEATHER
10	Light fog
28	Fog during the past hour, but NOT at time of observation.
41	Fog in patches
42	Fog, sky discernible, has become thinner during the past hour
44	Fog, sky discernible, no appreciable change during the past hour
46	Fog, sky discernable, has begun or become thicker during the past hour
43	Fog, sky NOT discernible, has become thinner during the past hour
45	Fog, sky NOT discernible, no appreciable change during the past hour
47	Fog, sky NOT discernible, has begun or become thicker during the past hour
50	Intermittent drizzle (NOT freezing) slight at time of observation
51	Continuous drizzle (NOT freezing) slight at time of observation

Tables 3, 4 and 5 summarize the fog data sets and are organized as follows. There is a table for each of the three basic inversion types shown in Fig. 1. Within each basic type, the strong inversion cases are presented first, followed by the weak. The definition of strong versus weak is based on the rate of temperature increase with height in the capping inversion. In the Type 3 inversion cases, we have included a category labeled 3N, for neutral, in which there was no capping inversion present, at least up through 850 mb. However, the surface layer was more unstable than the rest of the BL.

Within each of these groupings the cases are presented in order of increasing visibility. Within visibility levels, the cases are ordered by fog intensity: with sky NOT discernible coming first, then sky discernible, then drizzle conditions, then light fog, and finally, fog during the past hour.

The height of the inversion is given in millibars. For the Type 1 inversion, the first value is the sea level pressure, while the second value is the value at the top of the strong increase in temperature, which is tabulated in the intensity column. For the Type 2 inversion, the first line under the height column contains the sea level pressure and the top of the weakly inverted layer, with the corresponding temperature change in the intensity column. The second line gives the height at the top of the overlying increase in temperature, again with the value of this increase in the intensity column. For the Type 3 inversion, the sea level pressure and the pressure at the top of the MBL are presented. For the 3N cases, the second pressure value represents the top of the more unstable surface layer. In the intensity column we present the magnitude of the temperature increase in the inversion above the BL, as well as the pressure at the top of the strong increase in temperature. The other columns are self explanatory.

Table. 3 Characteristics of Type 1-Inversion Fogs

Case No.	Inversion Type	Height(mb)	Intensity(C)	Fog Type	Fog Code	Vsby (n mi)	Ship	Date Time	Synoptic Situation
1	1S	1012-950	6.0	TF	45	.025	C	72081212	Ahead of shortwave trough
2	1S	1025-1015	2.5	TF	47	.025	J	73072700	Southerly flow, west side of anticyclogenesis
3	1S	1010-985	5.0	TAD	45	.10	C	73070400	Broad SSW flow between low and semi-permanent high
4	1S	1030-1010	4.0	TF	47	.10	C	73071612	Broad SSW flow northwest of semi-permanent high
5	1S	1028-1000	4.0	TF	45	.10	C	73071700	Broad SSW flow northwest of semi-permanent high
6	1S	1025-1010	2.5	TF	42	.10	J	73072612	Southerly flow, west side of anticyclogenesis
7	1S	1005-955	13.5	TAD	46	.50	B	73070300	Center of low
8	1S	1005-950	8.5	TAD	50	.025	B	73070612	Southerly flow behind NE moving shortwave trough
9	1S	1025-1000	5.0	TAD	51	.025	C	72061200	Broad SSW flow northwest of semi-permanent high
10	1S	1025-1000	4.5	TF	51	.025	C	73071600	Broad SSW flow northwest of semi-permanent high
11	1S	1025-985	3.0	TF	10	.50	C	73071512	Broad SSW flow northwest of semi-permanent high
12	1W	1018-1000	1.0	TF	45	.025	C	72072212	Broad southeasterly flow between low and high
13	1W	1015-945	5.0	COL	45	.10	C	72070300	Center of low
14	1W	1020-1000	1.0	TF	47	.10	D	73060212	Broad WSW flow north of semi-permanent high
15	1W	1012-975	3.0	TAD	45	.10	C	73070800	Broad SW flow north of semi-permanent high
16	1W	1020-935	4.5	TAD	45	.10	C	73071712	Broad SW flow north of semi-permanent high
17	1W	1018-940	4.0	TF	45	.10	C	72060912	Broad southerly flow NW of semi-permanent high
18	1W	1025-975	1.0	TF	47	.25	J	73072712	Southerly flow west of high
19	1W	1015-1000	1.0	TF	43	.25	C	72072312	Broad southeasterly flow between low and high
20	1W	1020-1000	1.0	TF	45	.25	C	72071912	Southeasterly flow on west side semi-permanent high

Table. 3 (Continued)

Case No.	Inversion Type	Height(mb)	Intensity(C)	Fog Type	Fog Code	Vsby (n mi)	Ship	Date Time	Synoptic Situation
21	1W	1025-1000	Isothermal	TDP	46	.25	J	73072800	Ahead of shortwave trough
22	1W	1015-1000	Isothermal	COL	50	.025	K	72072312	Center of low
23	1W	1028-1000	0.5	TF	10	1.0	D	72061112	SSW flow north of semi-permanent high
24	1W	1025-1000	1.8	TF	28	2.0	D	73060300	Broad SW flow northwest of semi-permanent high

Table. 4 Characteristics of Type 2-Inversion Fogs

Case No.	Inversion Type	Height(mb)	Intensity(C)	Fog Type	Fog Code	Vsby (n mi)	Ship	Date Time	Synoptic Situation
1	2S	1026-1020 975	0.5 6.5	TAD	45	.025	C	72062300	Ahead of shortwave trough
2	2S	1029-1010 1000	1.0 3.5	TF	50	.025	J	72071612	Southerly flow, west side of anticyclogenesis
3	2S	1012-1000 970	0.5 6.0	TAD	45	.10	C	73070712	Crest of migratory ridge
4	2S	1024-1000 970	0.5 4.5	TAD	45	.10	C	73073012	Crest of migratory ridge
5	2S	1000-1003 915	Isothermal 11.0	TAD	45	.10	B	73070312	Center of low
6	2S	1024-1000 930	0.8 4.0	TAD	45	.10	C	73073100	Crest of migratory ridge
7	2S	1020-1000 965	0.5 4.0	TAD	43	.50	C	73080100	Crest of migratory ridge
8	2S	1008-1000 987	0.3 6.0	TAD	10	2.0	B	72070300	Ahead of shortwave trough
9	2S	1000-990 960	0.5 10.0	TAD	28	5.0	B	73070700	Crest of migratory ridge
10	2W	1010-975 940	Isothermal 1.0	TF	47	.025	M	73070212	Southerly flow ahead of northerly moving shortwave
11	2W	1031-1000 990	2.5 3.0	TF	45	.025	J	72071700	Southerly flow, west side of anticyclogenesis
12	2W	1016-985 905	Isothermal 3.5	TDP	47	.10	I	73071112	Ahead of shortwave trough
13	2W	1008-1000 975	0.2 3.0	TAD	45	.10	C	72072412	Broad southeasterly flow between low and high
14	2W	1018-1000 960	0.5 2.5	TAD	45	.10	C	73080112	Ahead of shortwave trough
15	2W	1024-1000 945	Isothermal 2.0	TAD	45	.10	C	73071200	Ahead of shortwave trough
16	2W	1015-1000 895	Isothermal 5.5	TAD	10	2.0	C	72061012	Shortwave trough line

Table. 5 Characteristics of Type 3-Inversion Fogs

Case No.	Inversion Type	Height(mb)	Intensity(C)	Fog Type	Fog Code	Vsby (n mi)	Ship	Date Time	Synoptic Situation
1	3S	1028-1013	5.5(990)	ST	47	.025	J	72071800	NE flow, east side of high
2	3S	1025-990	5.0(970)	ST	47	.025	J	72071912	NE flow, east side of high
3	3S	1030-1020	5.0(985)	ST	46	.025	J	72071600	S flow, west side of anti-cyclogenesis
4	3S	1022-1000	5.0(985)	TDP	45	.025	C	72062212	Ahead of shortwave trough
5	3S	1025-1000	7.0(960)	TDP	45	.025	C	72061112	Ahead of shortwave trough
6	3S	1025-1009	2.5(1000)	ST	47	.10	J	72071812	NE flow, east side of high
7	3S	1024-1000	5.5(980)	ST	46	.10	J	72071900	NE flow, east side of high
8	3S	1022-1000	4.5(980)	TDP	45	.10	C	73073112	Ahead of shortwave trough
9	3S	1000-980	6.0(970)	TDP	45	.10	B	72070312	Ahead of shortwave trough
10	3S	1027-1013	7.0(980)	TDP	44	.10	I	72071712	Ahead of shortwave trough
11	3S	1030-1004	5.0(995)	ST	42	.10	J	72071712	NE flow, east side of high
12	3S	1025-1000	4.5(970)	TDP	50	.025	I	72071800	Ahead of shortwave trough
13	3S	1015-980	4.0(940)	TDP	50	.025	J	72062312	Ahead of shortwave trough
14	3S	1020-985	4.0(965)	TDP	51	.25	J	73071000	Ahead of shortwave trough
15	3S	1010-1000	15.0(980)	TDP	10	2.0	B	72070212	Ahead of shortwave trough
16	3S	993-980	5.0(910)	COL	10	2.0	B	73071012	Center of low
17	3S	1005-995	6.0(850)	COL	10	2.0	B	73070400	Center of low
18	3S	1020-955	3.0(940)	TAD	28	0.5	J	73070912	Crest of migratory ridge
19	3S	1009-990	7.0(970)	TAD	28	1.0	I	73070912	Crest of migratory ridge
20	3W	1009-975	3.5(955)	TDP	46	.10	I	73071000	Ahead of shortwave trough
21	3W	1009-970	1.5(950)	TDP	44	.10	I	73071012	Ahead of shortwave trough
22	3W	1018-955	1.0(930)	TDP	45	.10	C	73080212	Ahead of shortwave trough
23	3W	980-970	3.0(850)	TDP	51	.10	B	73070712	Center of low
24	3W	1005-955	1.0(905)	COL	41	.25	I	73071812	Center of low
25	3W	1000-980	2.5(950)	TDP	10	.50	C	73070412	Ahead of shortwave trough
26	3W	1015-990	1.5(960)	TAD	10	.50	I	73071100	Crest of migratory ridge
27	3W	1010-990	1.0(960)	TAD	10	.50	I	72081212	Crest of migratory ridge
28	3W	1000-970	2.0(910)	TAD	10	.50	B	73072612	Shortwave trough line
29	3W	1024-980	2.5(850)	ST	10	2.0	J	72072000	NE flow, east side of high
30	3W	1013-900	4.0(850)	COL	28	1.0	I	73073100	Center of low
31	3N	996-970	--------	TAD	47	.025	I	72081112	Center of low
32	3N	1010-985	--------	COL	46	.10	I	73080100	Center of low
33	3N	1015-1000	--------	COL	43	.10	K	72072400	Center of low
34	3N	1015-1000	--------	TAD	50	.025	J	72070312	Shortwave trough line
35	3N	1025-1000	--------	TAD	10	1.0	K	73072512	NE flow, east side of anticyclogenesis
36	3N	1016-975	--------	COL	10	2.0	K	72072412	Center of Low

4. RATIONALE USED IN APPLICATION OF THE PHYSICS OF FOG FORMATION AND DISSIPATION TO FOG FORECASTING

4.1 Taylor Fog

Taylor fog is the predominant fog type in the N. Atlantic in the summertime. A large north-south gradient in SST exists north of 40 N, with the most intense gradient located west of 40 W at the confluence of the northward flowing Gulf Stream and southward flowing Labrador Current. The semi-permanent subtropical high is centered along 35 N, and thus the southerly flow at the western end of the high is located in the region of strongest SST gradient. In addition, this southerly flow has been conditioned by a long residence time over the ocean so that the low levels are characterized by relatively small dew point depressions. The initial and boundary conditions are therefore ideal for the formation of Taylor fog as the warm, moist air moves northward over the progressively colder ocean water.

4.1.1 Taylor Fog Formation

Obviously, fog cannot form in this air until the temperature is cooled at least to the initial dewpoint. In fact, it must be cooled somewhat further since, as the air is cooled, it also loses moisture to the sea surface which is colder than the surface dewpoint. No simple formulism exists for determining how far below the initial dewpoint the surface air must be cooled for fog to form. Undoubtably, the value varies from case to case, probably depending on the initial vertical profiles of temperature and moisture as well as the time history of the heat and moisture transfer rates in the inverted profile conditions which develop.

Detailed Lagrangian measurements of the vertical profiles of temperature and moisture, as taken during Taylor fog formation, do not exist. Observational studies have provided temperature and dewpoint profiles in and above Taylor fog (Taylor (1917), Emmons (1947), Mack and Katz (1976) and Rogers (1988)), and then make the observation that the temperature and dewpoint values in fog are less than the conditions found upwind of the gradient in SST. However, the conditions present at the instant of fog formation are not known.

A rule-of-thumb has been developed for this fog type through a limited, synoptic-type climatology. The scope of our research did not include pursuing traditional climatologies, which would not have provided the level of detail required for our analysis.

Examination of the episodes of Taylor fog contained in our data set showed that the warm, moist air upwind and south of the strong gradient in SST had surface temperatures in the 20-25 C range, with dewpoint depressions of the order of 2-4 C. Taylor fog appears to form in this air when the temperature cools on the order of 5 C; i.e., this value can be thought of as indicating that 2 degrees of cooling is not enough and 10 degrees is more than adequate. Since the 5 degree value is based on only gross, although useful, comparisons of quasi-homogeneous conditions in the nonfoggy and foggy air, we do not recommend using it as an absolute threshold. Rather, it could best be thought of as an estimate of the cooling value corresponding to a 50-50 chance of Taylor fog formation.

The location at which the physical processes related to fog formation are taking place are often best indicated by satellite data, which obviously should be used in fog forecasting. Prior to the formation of dense, continuous fog, the warm moist air flow is characterized by clear or scattered to broken cumuliform type cloud cover, which may be indictative of patchy fog. At the upwind edge of the fog formation region, this cloudiness becomes overcast stratiform (Gurka et al., 1982).

4.1.2 Taylor Fog Deepening

North of the major Taylor fog formation region (40-50 N) lies the west to east storm track followed by transient lows and troughs. Ahead of these features, southerly flow taps the pre-existing Taylor fog to the south and moves it northward into the upward vertical motion field located ahead of the system. In response to the upward vertical motion, the MBL thickens, the inversion rises and the lapse rate progresses from strongly inverted to weakly inverted to lapsed. Fog continues to exist in this deepening BL, although the visibility tends to increase as the layer deepens and the temperature profile becomes lapsed. An example of this transition is found in Fig. 2 which shows the changing vertical profile and fog intensity as the trough passed by the ship.

A key feature of the AESOP rule base is the type, intensity and height of the inversion in the vertical profile of temperature. An MBL with a lapsed profile and capped by an inversion with a height of less than 400 m had been found to be a necessary, but not sufficient, condition for stratus lowering fog

	WIND dddff	VSBY	SYNOPTIC SITUATION
(1) 7/4/73 00Z	24023	1/8 n mi	Fog; flow around high cell
(2) 7/4/73 12Z	24020	1/2 n mi	Light Fog; flow ahead of shortwave trough
(3) 7/5/73 00Z	02014	5 n mi	Drizzle; flow behind shortwave trough

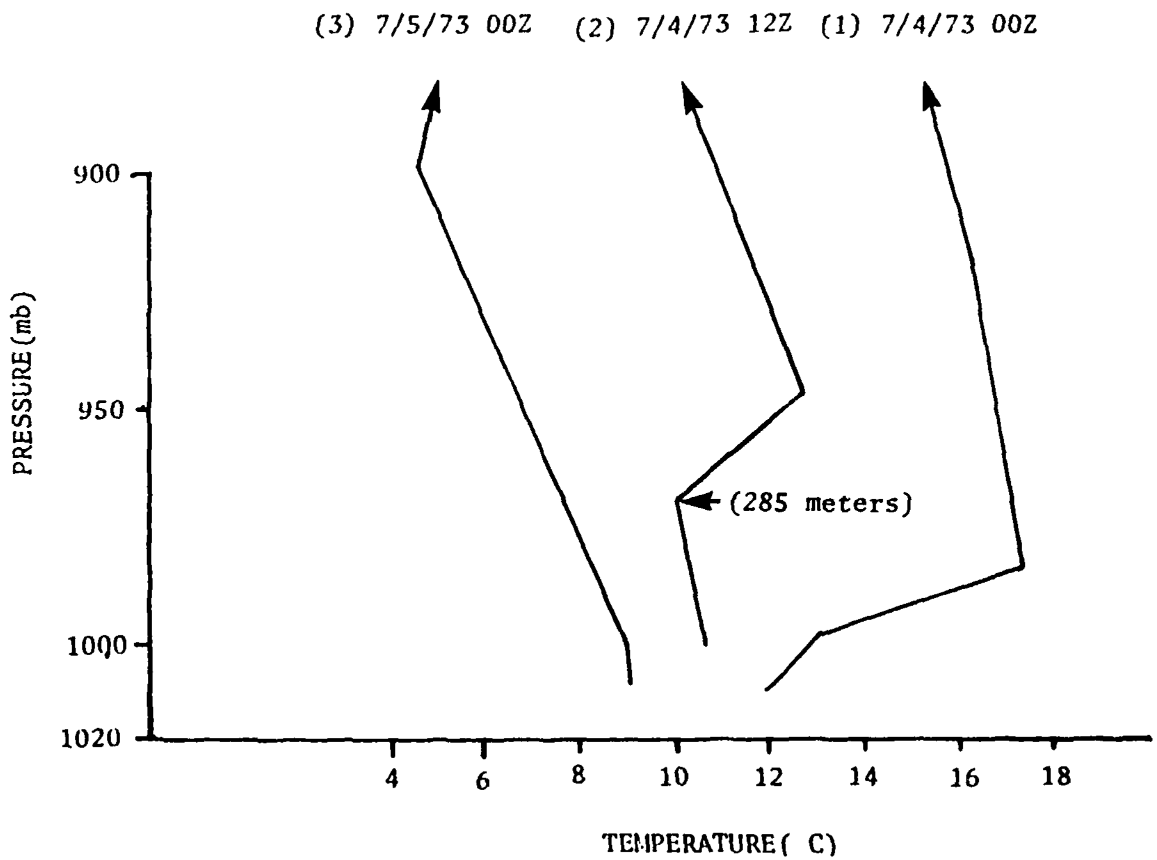

Figure 2. Example of Taylor deepening fog at Ocean Station 4YC.

to occur off the west coast of the United States. The initial AESOP rule base contained this criterion for stratus lowering fog while being unaware of the similar conditions accompanying Taylor-deepening fog. Thus, the test forecast made from 1200 GMT in Fig. 2 correctly predicted fog (inversion height of 285 m), although this was not a case of stratus lowering fog. However, because a Taylor-deepening fog can occur with inversions somewhat greater than 400 m, a knowledge of the potential fog type (assessed from the synoptic flow patterns) must be included in the rule base to allow Taylor fog to be forecast for these higher inversions. Also, the Taylor-deepening fog does not tend to dissipate during midday as stratus lowering fog does. So, the distinction between these two fog types needs to be made for purposes of fog dissipation as well.

4.1.3 Taylor Fog Dissipation

On a large scale, dissipation of Taylor fog seems to be the end result of the BL deepening process discussed above. The previously-formed fog is drawn into the upward vertical motion field located ahead of a cyclonic system. Depending on the intensity and duration of the vertical motion, and the continued cooling of the air at the ocean surface, the fog dissipates. Our observations suggest that an inversion height of 700 m may represent the deepest layer in which fog can be maintained. We therefore recommend that fog dissipation be forecast for that time when the inversion height is expected to exceed that height.

4.1.3.1 Heating by the Ocean Surface

Taylor fog can also dissipate through either heating from the surface or from mixing in of warm, dry air from above the fog top. Both processes were observed during the 1975 Nova Scotia cruise (Mack and Katz, 1976), coincidentally for a fog observed on 5 August 1975. (Complete data for this fog are presented in the referenced report on pages 18-25 and A-49 through A-53.) During this period, the ship was steaming into the wind along a WNW heading. The SST pattern, and the vertical temperature and visibility time series, are shown, respectively, in Figs. 3 and 4. The water temperature pattern is characterized by a 12 n mi wide cold pool, with a six degree increase in temperature occurring over the space of six n mi at its downwind edge. The air temperature is cooled to a height of 17 m as the air moves over the cold pool, producing a 1 C inversion between 17 and 28 m. The air temperature starts to increase almost immediately after the water temperature increases, and then levels off about seven n mi downstream (~0340 EDT) as the visibility starts to increase rapidly.

Analysis of the vertical profile of temperature shows that the visibility begins to increase after the low level temperature inversion is destroyed, at approximately 0340. At this time the low-level temperature also ceases to increase, which is consistent with the export of heat out of the low levels. Consequently, when the low-level temperature inversion is destroyed, the low levels become recoupled with the remainder of the MBL and the properties of the low levels are mixed throughout

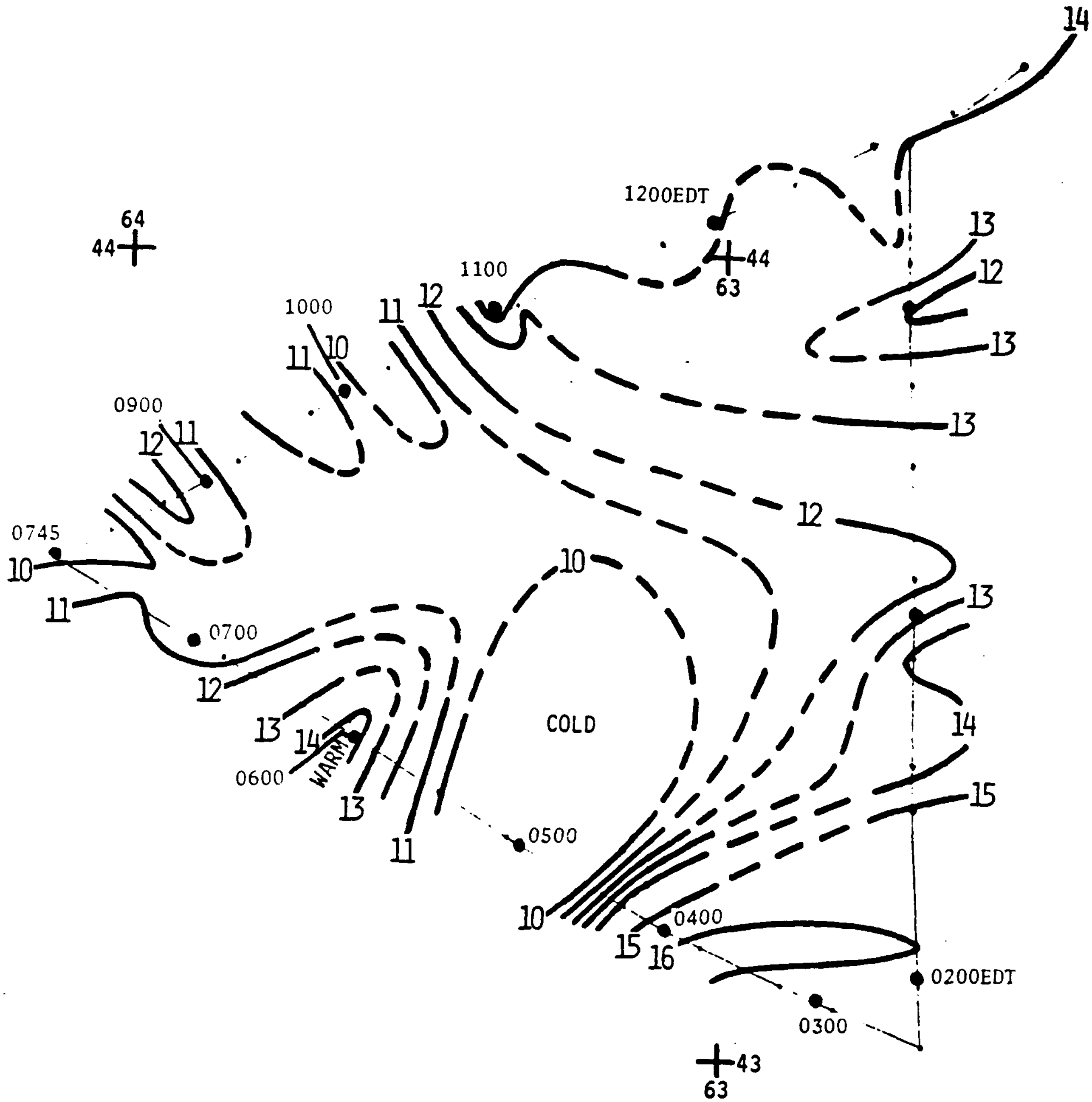

Figure 3. Sea surface isotherm (C) analysis for fog observed off Nova Scotia between 2200 and 1300 EDT, 4-5 August 1975 (see text).

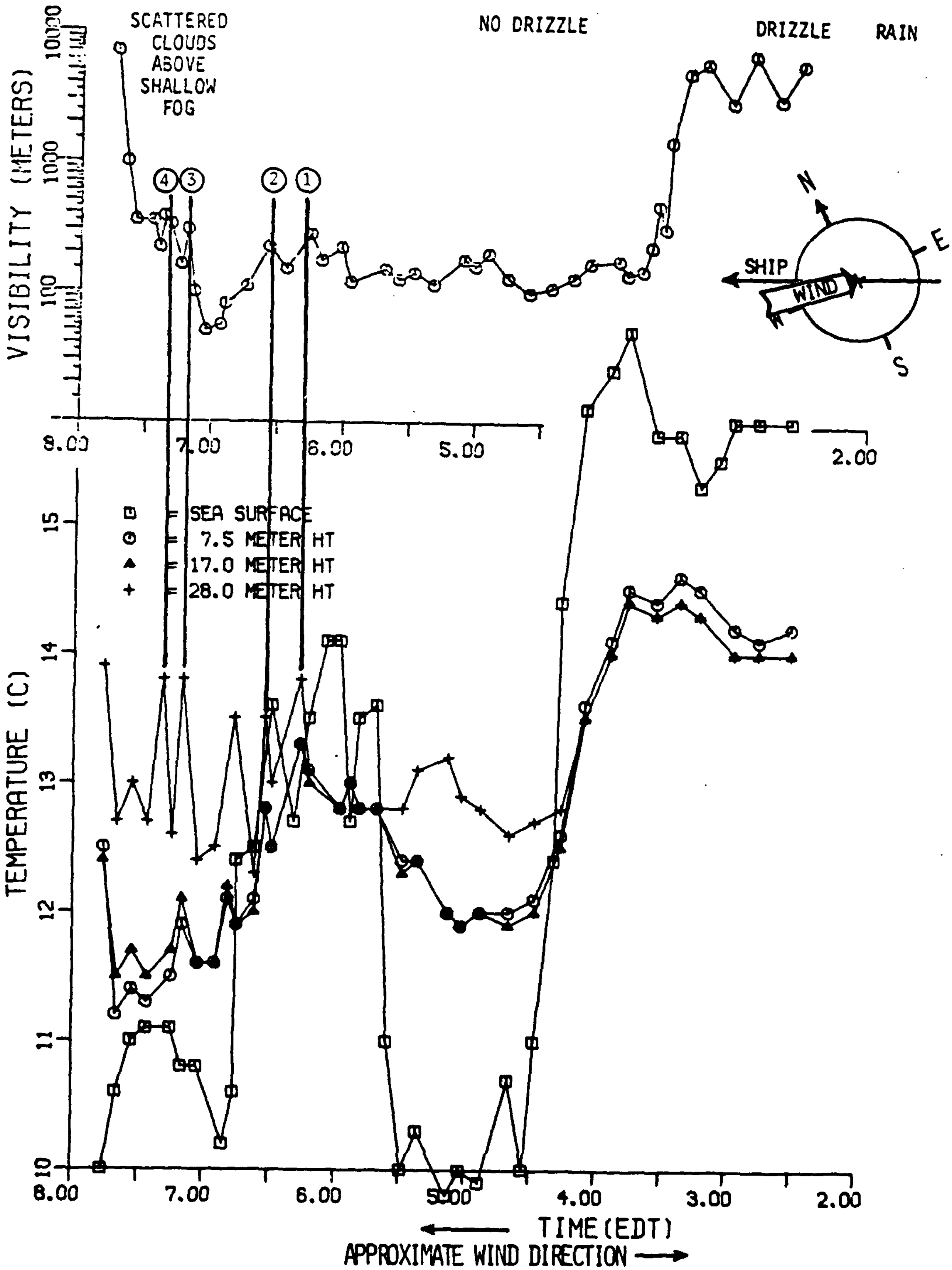

Figure 4. Visibility, water and air temperatures at 7.5,17 and 28 m heights, versus time for situation depicted in Fig. 3 (see text).

the BL.

Thus we find a fog contained in a relatively shallow, stable surface-based BL produced by cooling from the underlying cold ocean water. When this inversion is destroyed by strong heating associated with a large increase in SST, the shallow inverted layer becomes recoupled with the deeper, unsatured MBL and the fog dissipates by being mixed into the deeper layer. The fog analyzed above was indeed a Taylor fog, albeit one whose inverted temperature profile in the low levels was weak.

While the above analysis demonstrates a physical process that can cause dissipation of Taylor-type fogs, it is important to examine the climatology of the region to determine if that process is important to the fog forecasting system. Taylor fogs observed at locations like 4YC, where the air has a long history of cooling, have inverted, saturated profiles of 5 C extending through 250 m. The five degree increase in ocean temperature needed to make the profile isothermal would require the air to move southward toward the northern edge of the Gulf Stream. As mentioned earlier, the synoptic flow patterns existent in the N. Atlantic in the summertime produce this southerly motion almost exclusively behind fronts and troughs in air which is not initially foggy. Thus, dissipation of Taylor fog by heating from the ocean surface almost never occurs in the N. Atlantic, except for the shallow Taylor fogs formed over local cold pools as observed in the example above off Nova Scotia.

4.1.3.2 Intermixing of Warm, Dry Air

Mixing of warm, dry air from above the inversion into the foggy MBL is a mechanism for fog dissipation. This process has been studied extensively by Telford and his colleagues (Telford and Keck, 1988; Telford and Chai, 1984), primarily in connection with dissipation of a stratus deck which caps a marine boundary layer. Some evidence exists that this process acts on Taylor-type fogs as well, particularly where the inversion is near the ocean surface. Such a situation was observed toward the end of the fog case discussed above in Section 4.1.3.1.

The fluctuations in the 28 m temperature from 0630 to 0730 represent measurements taken in the cloud (cold) and clear air (warm) regions present along the corrugated top of the fog. The warm (clear) regions appear to be areas where warm, dry air is being mixed into the foggy air below. Note the correlation in Fig. 4 between the peaks in visibility, labeled (1) through (4), and the corresponding peaks in the 28 m temperature. In this situation the fog is not completely dissipated, probably because the process has just started; the large scale dynamics has only recently brought the inversion down to near the surface.

After emerging from the shallow continuous fog at 0745 the ship changed heading to the ENE; the temperature data along this track are shown in Fig. 5. The 28 m temperature showed a steady increase during the three hour period, with fluctuations to lower values as shallow fogs associated with cold tongues of water continued to be encountered.

After 1000 the 7.5 and 17 m temperatures increased rapidly

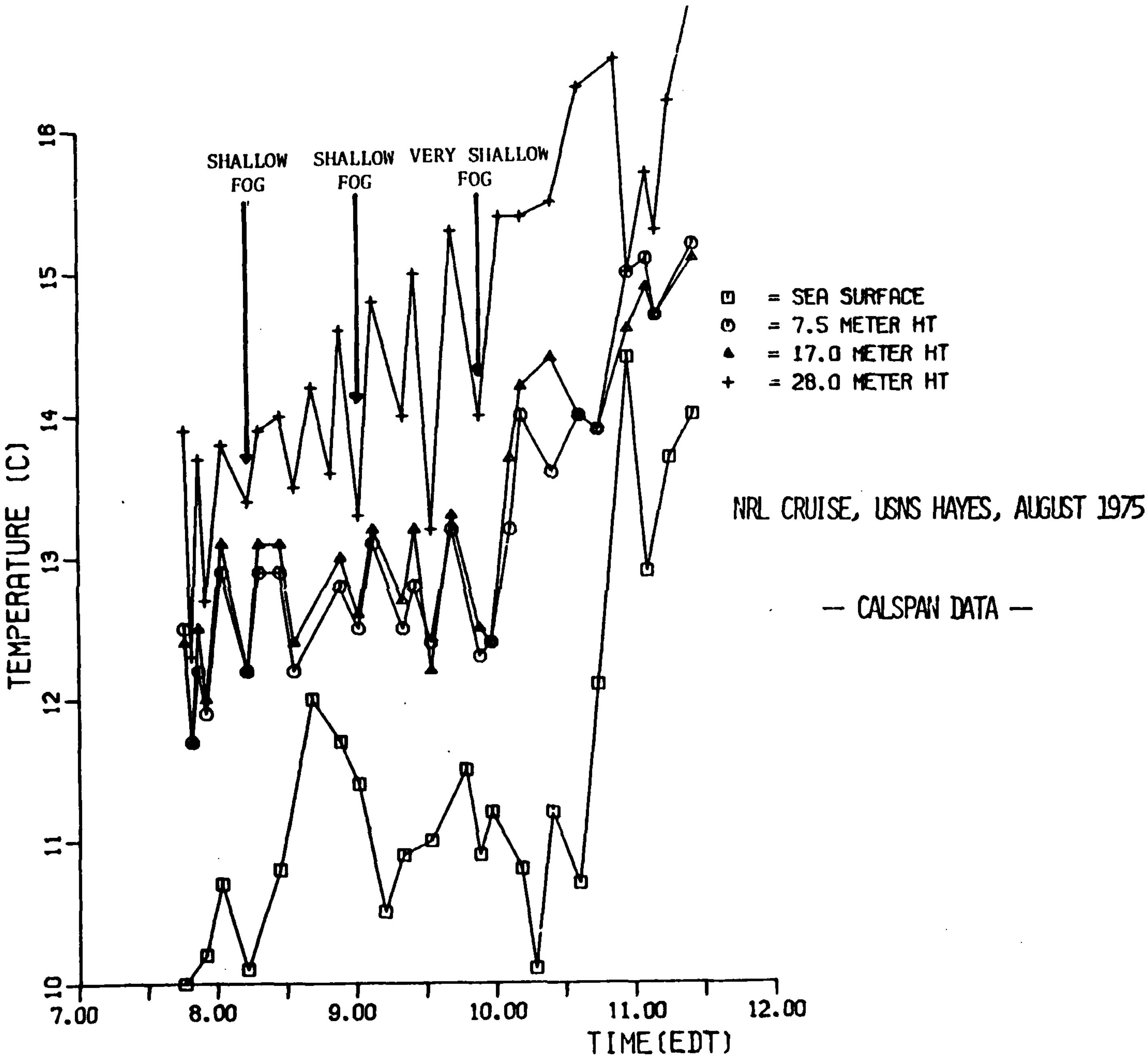

Figure 5. Air and sea surface temperatures vs. time--5 August 1975, off the coast of Nova Scotia (see text).

as the inversion was pushed down to these levels. A vertical sounding taken from the ship around 0945 showed the inversion extending to 200 m. After 1000, the temperature profile observed in the lowest 28 m is consistent with adiabatic descent of the temperature profile measured higher in the ship sounding. Although cold tongues of water continued to be encountered, fog was not observed after this time, probably because the inversion had been lowered to very near the ocean surface.

What is the application of this concept to dissipation of Taylor fog over the open ocean? A class of Taylor fogs was observed in the data set in which the inverted profile from the surface was weak, on the order of 0.5 to 1.0 C in 100 m. These fogs were found where the air had experienced weak cooling by the ocean surface; e.g., at 4YD where the basic gradient in SST is small and at 4YC with an east-southeast wind which crosses the SST isotherms from warm to cold at about 30°.

AESOP forecasts made from these cases showed both fog persistence and dissipation accompanied by little change in inversion strength. The key to this apparent dichotomous behaviour lies in whether or not warm, dry air is available in the inversion above the fog for mixing into the fog. If the dew point depression at 1000 mb is greater than or equal to 2 C, then fog dissipation is likely, particularly if the six-hour forecast period is during daylight. If the dew point depression is less than 2 degrees, then fog persistence is more likely. These rules should be included in the AESOP semantic net for situations in which the cooling of the air by the ocean is small.

4.2 Stratus Lowering Fog

Stratus lowering fog is the prevalent fog type off the west coast of the United States during the summertime. It was the subject of numerous field trips conducted and led by Calspan Corp. in this region during the 1970's. In Rogers et al. (1981) stratus lowering fog was the main constituent of an experimental decision tree developed at Calspan for forecasting west coast fog. During a 1975 U.S. Navy cruise, stratus lowering fog was found to occur in the N. Atlantic off the coast of Nova Scotia (Mack and Katz, 1976). It was first documented to occur over higher latitude open ocean regions in a case study for Ocean Weather Ship Papa (50N,145W) in the eastern Pacific (Clark, 1981). Rogers (1988) found numerous cases of stratus lowering fog associated with anticyclogenesis at higher latitudes in the eastern N. Atlantic.

4.2.1 Formation of Stratus Lowering Fog

The physics of stratus lowering fog is fairly well documented, understood and reproduced by numerical simulation (Oliver et al., 1978; Mack et al., 1983). This fog forms at night in an MBL capped by a stratus deck. As the sun sets, because long wave radiative cooling is no longer counteracted by solar radiation near the stratus top, the layer cools. In response to this cooling the base of the stratus lowers to the ocean surface, producing fog. A BL of less than or equal to 400 m thickness has been found to be a necessary, but not sufficient, condition for formation of stratus lowering fog; however, occurrence of this fog type is extremely high when the inversion

is below 400 m. The reason this threshold depth is not a sufficient condition is because heating from the ocean surface, and entrainment of warm, dry air across the capping inversion, can counteract the long wave cooling.

Prevention of fog formation by heating by the ocean is relatively rare. The surface air temperature is frequently equal to the SST. If colder than the SST, the air temperature is usually within a couple of degrees Celsius of the water temperature, thus providing small heat tranfer to the boundary layer.

On the other hand, entrainment of warm, dry air across the capping inversion is potentially a more important fog prevention process. Lilly (1968), in his theoretical study of cloud-topped mixed layers, noted that an upward increase in wet bulb potentiial temperature above cloud top was needed for stability of the cloud top against penetration by the very dry air located in the overlying inversion. Recently, Telford and Keck (1988) have featured the vertical profile of wet bulb potential temperature in analysis of a number of field studies of entrainment across an inversion capping a stratus deck. For entrainment to occur, the wet bulb potential temperature must decrease with height across the inversion.

The profile of wet bulb potential temperature can be determined from the temperature and dewpoint profiles on a thermodynamic chart. First, from these two temperatures at any level, the lifting condensation level can be determined in the standard fashion by finding where the dry adiabat and the

constant mixing ratio lines intersect. Then, proceeding along the moist adiabat through this intersection point to 1000 mb determines the adiabatic wet bulb potential temperature for the original level. For most practical applications the adiabatic wet bulb potential temperature is a good approximation to the wet bulb potential temperature. A description of this analysis can be found in Petterssen (1956). An illustration of the application of this type of analysis to fog forecasting is presented below.

This temperature criterion was applied to a situation observed during CEWCOM 76 (Cooperative Experiment in West Coast Oceanography and Meteorology-1976) , a situation which has heretofore always been thought not to have had fog because of mixing of warm, dry air from above the inversion. On the evening of 9 October 1976, the R/V ACANIA was underneath a broken stratus cloud deck located some 70 n mi west of Vandenberg AFB, with satellite observations indicating no accompanying middle or high clouds. A sounding taken at 1708 PDT indicated the inversion was located at 293 m. The ship steamed east-northeastward during the night and no fog occurred. A sounding taken at the eastern end of the track at 0630 PDT showed the inversion still below 400 m, at 370 m. Thus, no fog occurred although the inversion remained below 400 m for the entire night.

The analysis of the wet bulb potential temperature profiles for both soundings indicated a decrease of temperature above the stratus top; therefore, Telford and Keck's theory predicts a mixing of warm, dry air down into the stratus deck. Because the

air was on the order of 1 C colder than the water, the major deterrent to fog formation appears to have been the mixing in of warm, dry air.

Conversely, stratus lowering fogs show an increase of wet bulb potential temperature with height above the top of the cloud, and thus mixing of warm, dry air into the stratus cloud does not occur, in general.

If conditions otherwise indicate the likelihood of stratus lowering fog, except for the presence of entrainment of warm dry air across the inversion, AESOP should forecast stratus lowering fog; however, the probability should be around 75% rather than 100%.

4.2.2 Dissipation of Stratus Lowering Fog

Dissipation of stratus lowering fog occurs during the daytime when the solar heating within the cloud offsets the long wave radiative cooling at the cloud top. Observations indicate that for mid latitudes, solar radiation is strong enough to effect dissipation during the early morning hours. However, we discovered that several AESOP test cases involving stratus lowering fogs at high latitudes showed no fog dissipation during the daytime. Analysis of these cases by the designer and developer of AESOP, J. Peak of Martin Marietta Data Systems, indicated that a solar elevation angle greater than 30° is required for dissipation of stratus lowering fog. In addition, the numerical simulation of Oliver et al. (1978), for summer solstice at 40 N, suggests that fog dissipates about 3 hours after sunrise when the solar elevation angle is 40°

above the horizon. During CEWCOM 76, a stratus lowering fog was observed on 13 October 1976 at 33 N. This fog did not dissipate until after 1100 LDT when the solar elevation angle rose above 40°. Thus, we propose using a solar elevation angle of 40° as a threshold for dissipation of stratus lowering type fog.

4.3 Fog At the Center of Slowly Moving Low Centers

Like Taylor deepening fog, this fog type was not delineated until analysis was made of the forecast failures from the preliminary test of AESOP. Of the seven AESOP test cases in which fog occurred but was not forecast, four cases occurred near the center of a slowly moving low center. Of these four, three were located around 60 N in the eastern N. Atlantic, where quasi-stationary closed lows are frequently located.

Inversion heights and MBL depths in the 600-700 m range are associated with these fogs. Visibilities are near the upper end of the fog range, 1/2 to 1 n mi. Two fog formation processes appear to operate here. With a very nearly saturated MBL and almost calm winds, the weak radiational cooling present is sufficient to form fog in the late evening, similar to fog formation which occurs near the center of quasi-stationary lows over land. In contrast to these cases involving a deep, nearly saturated MBL, fog can also form in the near-surface, nearly saturated layer that can result from cooling by small pools of cold water; Mack and Katz (1976) observed such pools and the associated fog formation process off the coast of Nova Scotia in 1975.

In addition, one can find a mixture of Taylor deepening fog and fog near the center of a slow moving low--when the timing and location are such that pre-existing Taylor fog is drawn quickly into a low center that is closing off and slowing down. In these cases, the inversion is lower than the 600-700 m mentioned above, but still above the 400 m threshold used for forecasting the occurrence of stratus lowering fog. Again we see the importance of both the synoptic situation and the history of the air containing the fog in making a proper classification of the fog type.

5. HAZE FORMATION AND DISSIPATION

As stated earlier, haze, for the purposes of this study which used ocean ship weather reports, is defined as a visibility greater than 1 n mi amd less than or equal to 5 n mi, with no precipitation occurring. The lower limit arises from our definition of maximum visibility in fog, and the upper limit arises from the resolution in visibility of the ship weather code, i.e., 2, 5 and 10 n mi. Because ten n mi visibility is too large to be considered as the upper limit for haze occurrence, we use 5 n mi.

The investigation of haze formation and dissipation was carried out during Task II (Year 2). Haze formation was examined from the standpoint of both 1) deliquescence and subsequent growth of aerosols as relative humidity increases from moderate to high values (>90%), and 2) a condition which occurs either before fog formation or after fog dissipation. With regard to the former, we found that over the open ocean, at least 1500 km from the coast (and even with offshore winds), the aerosol concentration is generally too small to reduce the visibility to the 5 n mi upper limit of haze, even at high relative humidities!

Certain geographical sites show a high frequency of haze at times. The Gulf of Oman shows haze during July and August when both the aerosol concentration and relative humidity are high enough to produce haze visibility levels (McGee,1989). In addition, observations taken in the interior of the Mediterranean Sea (Mack et al., 1978) show that the aerosol concentration is

large enough for haze to form at the very high relative humidities.

For haze occurrence in the context of fog life cycles, we found that haze most frequently occurs over both short distances and times; so, haze is a relatively rare occurrence when associated with fog. We noted two exceptions to this finding. One is in the dissipation of stratus lowering fog for situations in which the solar elevation angle takes a relatively long time (>1hr) to climb from 30 to 45^{o}. The second occurs with light, embryonic Taylor-type fogs which form when the SST gradient along the wind direction is weak. In both these exceptions, visibilities in the haze range may occur for as long as a couple of hours.

5.1 <u>Open Ocean Haze Formed by Aerosol Deliquesence and Growth</u>

Our analysis is based on aerosol concentration data acquired during two transatlantic cruises, one across the mid-latitudes (45-35 N) in May 1977 (Mack et al., 1978), and the other across the subtropical Atlantic (30-20 N) in March 1983 (Wattle et al., 1983 and Hoppel et al., 1988). The first cruise took ten days and the second one took almost three weeks to transit the Atlantic.

On neither of these cruises did the visibility fall below the 5 n mi (9.25 km) haze threshold value, although relative humidity was above 90% on at least six of the days. During the 1977 cruise, the lowest visibility measured was 16 km, with a relative humidity near 95%; in 1983, the corresponding figures were 15 km with a relative humidity near 90%. Thus, even with

high relative humidities the visibilities were above the haze threshold, indicating that the aerosol concentration was low.

To investigate this result, we performed the following analysis. We computed the aerosol concentration needed to produce the haze visibility threshold, by assuming near optimum conditions for scattering, i.e., a monodisperse aerosol distribution at the particle diameter for which the Mie particle scattering coefficient is a maximum. The specific Mie curve we used was for a wavelength of 0.474 μm and a saturated NaCl solution with refractive index of 1.37 (Mack et al., 1978). The maximum particle scattering coefficient (k) of four occurs at a particle diameter of 0.8 μm. The equation relating the composite scattering coefficient, β_{SCAT}, to visibility (visual range), V, is

$$\beta_{SCAT} = \frac{3.912}{V} \tag{1}$$

and that relating concentration, n, to k and particle radius, r, is

$$n = \frac{\beta_{SCAT}}{\pi K (r)^2} \tag{2}$$

Eqs. (1) and (2) provide n = 210 cm^{-3} at 0.4 μm radius and V = 9.25 km.

Reference to the aerosol distributions measured on the two transatlantic cruises shows that the concentrations at this size are in the tens, rather than the 100's, per cubic centimeter, at the moderate (80%) relative humidity of the

observations. Although the concentrations at sizes somewhat smaller than 0.8 μm are in the 100's cm^{-3} range, these aerosols do not grow to the 0.8 μm diameter range even when the humidity is increased to 98% (Mack et al., 1978).

Another possibility for reducing the visibility to haze values is if the larger concentration values present at the smaller aerosol sizes compensate for their smaller particle scattering coefficient and geometrical cross section. The particle scattering coefficient is reduced to two at a diameter of 0.4 μm. The corresponding concentration required for a 9.25 km visibiiity is 1680 cm^{-3}. With the measured values in the 100 cm^{-3} range, the concentrations are again too small to produce a haze visibility.

A complete analysis of the potential for low visibility involves increasing the relative humidity and computing the change in radius over all aerosol sizes spanned by the measured size distribution. The resulting β_{SCAT} at a given relative humidity is computed by evaluating Eq. 2 for the individual size categories and then summing the results. The final product is a curve of visual range vs. relative humidity. In Mack et al. (1978) such a curve, prepared for an oceanic aerosol, required a relative humidity of 98% to produce a visibility of 10 km--suggesting imminent fog formation rather than haze.

The above computations were carried out using data acquired over the open ocean during the 1977 cruise. The numerous aerosol size distributions acquired over the open ocean during the 1983

cruise also show that the aerosol concentrations in the important size ranges were insufficient to produce haze visibility levels.

In summary, over the open ocean and at least 1500 km offshore, the aerosol concentration is so low that the haze visibility threshold of 5 n mi (9.25 km) cannot be produced, even at very high relative humidities. Although the distributions have peak concentrations of several 1000 cm^{-3}, these values occur at diameters of a few hundreths of a μm, where the geometric cross section is very small and the Mie particle scattering coefficent is essentially zero. At the larger diameters where geometric cross section and the Mie scattering coefficient both are larger, the concentrations are too low to produce haze.

5.2 Haze Formation within 1500 km of Continents (Offshore Flow)

Within 1500 km of the coast line in offshore flow, observations show the aerosol distribution to be representative of continental distributions, which are characterized by large particle concentrations (in comparison to marine aerosols). For westerly flow off the southeastern United States and easterly flow off the Iberian Peninsula, Hoppel et al. (1988) show concentrations in the 1000's cm^{-3} at 0.4 μm diameter and near 100 cm^{-3} at 0.8 μm diameter. Each of these monodisperse concentrations is sufficient (see computations above) to lower visibility to haze levels. Thus, the total aerosol distribution would probably produce haze visibility levels when brought to high relative humidity levels.

After crossing the Atlantic, the 1977 cruise continued into the Mediterranean Sea. An aerosol distribution taken some 200 km south of Malta under west-northwesterly flow off Africa to the west, showed a continental type distribution with more particles present above 1 μm diameter than observed over the ocean. A visibility vs. relative humidity curve prepared for this distribution showed that haze visibility levels would be reached at 97% relative humidity.

During a cruise in the Straits of Gibraltar in June 1986, Wattle (1987) observed visibilities in the 2-6 km range within a couple of kilometers of the Moroccan coast. These observations were taken in the early morning (0600 local time), with relative humidities around 90%. The corresponding β_{SCAT} of 2 km $^{-1}$ at this relative humidity is consistent with the results of Fitzgerald et al. (1982) for continental aerosols measured in Washington, D.C.

As can be seen from the above examples, haze visibility levels occur at different values of high relative humidity, depending on aerosol size distribution and chemical composition. Without direct measurement of these parameters it is difficult to predict the relative humidity at which haze visibilities will be reached. Since we know that relative humidity above 90% is required to produce haze visibilities in most natural, coastal oceanic aerosol populations, we propose using that value as a threshold for haze formation. With information about the history of the air in which the haze forecast is to be made, this threshold can be modified. If the air has had a recent

continental influence, then 90% is probably an appropriate value. The longer the air has been removed from continental sources, the higher the relative humidity has to be for haze to form. At the 1500 km limit, a value near 98% seems appropriate. As with other threshold numbers proposed in this study, these values should be looked upon as estimates that indicate a 50% probability of the phenomenon occurring.

6. CRITIQUE OF AESOP 1.0

Under Phase 1 of this contract, Calspan Corp. undertook a study of the formation of fog in the N. Atlantic in order to provide a basis for fog forecasting in that region (Rogers, 1988). These findings were incorporated, along with previous information about fog formation in the eastern Pacific, into a prototype expert system for fog prediction (AESOP) which was developed for NEPRF by Martin Marietta Data Systems (Peak, 1988). Under Phase 2 of this contract, Calspan Corp. critiqued the AESOP system to discern the reasons for inadequate forecasts, and to suggest refinements and additions to the forecasting rules. In particular, we expanded the AESOP rule base by examining fog dissipation as well as haze formation and dissipation.

The AESOP system was tested for the general time periods used in Phase 1 to study fog formation in the N. Atlantic. However, the forecasts were somewhat independent since the fog formation study used the observations taken at 0000 and 1200 GMT while the AESOP test made 6-hour forecasts verifying at 0600 and 1800 GMT. The results are found in Peak (1988). Of the 76 test cases, there were 29 incorrect forecasts, eight from clear, six from haze and 15 from fog initial conditions. Seven of these cases were not considered in our analysis because the reduction in visibility at the verification time was due to precipitation, and not fog or haze. Also, one correct forecast was erroneously categorized, and two forecast failures were caused by mistakes made either in the input data or in applying the forecast rules.

Finally, the reason for three forecast failures could not be determined from the time and space scales of the available data.

Of the remaining 22 forecast failures, 13 were related to specific synoptic effects:

1) Weather improvement, cold frontal passage (5).

2) Stationary low center (4)

3) Advection of pre-existing fog (2)

4) Taylor fog, but located <u>in</u> synoptic trough (2)

The first three situations were not considered under Phase 1 since we had focused on fog formation. Situation (1) above is fog clearing associated with a change in the air mass; Situation (2) is fog persistence and Situation (3) is movement of pre-existing fog, neither of which concern fog formation. Situation (4) was a high latitude (60^{o}) condition not encountered in the original study.

Three forecast failures were associated with solar effects. Two of these involved dissipation by heating of shallow Taylor fogs during the daylight hours. The other case involved a stratus-lowering type fog and nonrecognition by the system that for 20 W, 1800 GMT falls during the early evening and thus during the beginning of cooling by net longwave radiation.

All 16 of these "forecast failures" are related to influences which were not contained in the prototype AESOP system. Modification of the AESOP rule base by appropriate inclusion of these influences improved the AESOP performance. Consultation between the Calspan fog expert and the AESOP

developer indicated that these rules should be located at a high level in the semantic nets, as befits their importance.

Not only were the forecast failures examined, but correct forecasts were also examined, in particular those which required forecasts to form worse conditions, i.e., clear to haze (four cases) and haze to fog (16 cases). In the forecast of fog from haze, five of the cases were not considered since the reduction of visibility was due to precipitation. Of the remaining eleven only one had fog as a result of advection of pre-existing fog, while the other 10 fog occurrences followed the fog formation processes contained in the AESOP rule base. In the clear to haze situations, two of the cases were not considered, again due to the presence of precipitation. The other two cases appeared to follow the haze formation processes of the AESOP semantic nets. Thus, overall, the AESOP system seemed to work well when it was used for those situations of deteriorating visibility for which it was originally designed.

ACKNOWLEDGMENTS

The research described in this report is dedicated to Gene Mack, former head of the Atmospheric Sciences Section at Calspan who died suddenly in October 1986 when this work was still in the proposal stage. Without Gene's tireless efforts much of the field study data which form the basis for our understanding of fog life cycles would not have been acquired. Gene's goal and dream was some day to be able to describe all the various fog life cycles from field data. Gene realized his goal for the stratus-lowering fog type, since it was fairly well documented and understood by virtue of the eight field programs which he led and participated in along the west coast of the United States in the 1970's. However, the Taylor-type fog of the western North Atlantic escaped Gene's detailed and intensive scrutiny. Of the three N. Atlantic cruises which Gene was involved with in the 70's and 80's, the two transatlantic cruises met with no fog. Only the 1975 cruise off the south coast of Nova Scotia encountered fog, and this field study was severely handicapped by the inability to direct the ship's course to provide optimum data. It was only through diligence, imagination and extremely meticulous analysis that Gene was able to glean any insight at all into Taylor fog processes from these data. We hope the descriptions of fog life cycle presented here, which are based both on the N. Atlantic data acquired for this study and on further analysis of the Nova Scotia data, provide in large measure a solid first step toward achieving Gene's lifelong goal.

I would like to thank Bruce Wattle for many discussions during this work, which clarified my perceptions, particularly in the measurement of aerosol concentrations. Roland Pilie deserves much thanks for his continual guidance and support during the program. Finally, a special acknowledgment goes to Dr. P. Tag, the program COTR, for his thorough review of the manuscript and incisive suggestions for it's clarification and improvemnt.

REFERENCES

Clark, R.J., 1981: "An Open Ocean Marine Fog Development and Forecast Model for Ocean Weather Station PAPA." Naval Postgraduate School Thesis, Naval Postgraduate School, Monterey CA 93943, 129 pp.

Emmons, G., 1947: "Vertical Distributions of Temperature and Humidity Over the Ocean Between Nantucket and New Jersey." Papers in Physical Oceanography and Meteorology, Vol. X, No. 3. Massachusetts Institute of Technology and Woods Hole Oceanographic Institution. Cambridge MA 02139 and Woods Hole MA 01784, December 1947, 89 pp.

Fitzgerald, J.W., W.A. Hoppel and M.A. Vietti, 1982: "The Size and Scattering Coefficient of Urban Aerosol Particles at Washington, DC as a Function of Relatvie Humidity." J. Atmos. Sci., 39, 1838-1852.

Gurka, J.J., V.J. Oliver and E.M. Maturi, 1982: "The Use of Geostationary Satellite Imagery for Observing and Forecasting Movement of New England Sea Fog." Preprint Volume, 9th Conference on Weather Forecasting and Analysis, June 28-July 1, 1982; Seattle, WA. Published by American Meteorological Society, Boston MA 02108, 143-151.

Hoppel, W.A., J.W. Fitzgerald, G.M. Frick and R.E. Larson and E.J. Mack, 1988: "Atmospheric Aerosol Size Distributions and Optical Properties Found in the Marine Boundary Layer over the Atlantic Ocean." Naval Research Laboratory, Washington, DC 20375-5000 and Calspan Corp. PO Box 400, Buffalo NY 14225, December 1988, 120 pp.

Lilly, D.K., 1968: "Models of Cloud-topped Mixed Layers Under a Strong Inversion." Quart. J. Roy. Meteor. Soc., 94, 292-309.

Mack, E.J., Anderson, R.J., Akers, C.K. and T.A. Niziol, 1978: "Aerosol Characteristics of the Marine Boundary Layer of the North Atlantic and Mediterranean during May-June 1977." Project SEA FOG: Sixth Annual Summary Report, Calspan Report No. 6232-M-1, October 1978, 215 pp. Calspan Corp., P.O. Box 400, Buffalo, NY 14225.

Mack, E.J. and U. Katz, 1976: "The Characteristics of Marine Fog Occurring off the Coast of Nova Scotia." Project Sea Fog Fourth Annual Summary Report-Part 1, Calspan Report No. CJ-5756-M-1, Contract No. N00019-75-C-0508, June 1976, 181 pp. Calspan Corp., P.O. Box 400, Buffalo, NY 14225.

Mack, E.J., U. Katz, C.W. Rogers, D.W. Gaucher, K.R. Piech, C.K. Akers and R.J. Pilie, 1977: "An Investigation of the Meteorology, Physics and Chemistry of Marine Boundary Layers Processes." Project SEA FOG: Fifth Annual Summary Report, Calspan Report No. CJ-6017-M-1, October 1977, 122 pp. Calspan Corp., P.O. Box 400, Buffalo, NY 14225.

Mack, E.J., and T.A. Niziol, 1978: "Reduced Data From Calspan's Participation in the CEWCOM-78 Field Experiment Off the Coast of Southern California During May 1978." Project SEA FOG: Sixth Annual Summary Report, Calspan Report No. 6232-M-2, October 1978, 97 pp. Calspan Corp., P.O. Box 400, Buffalo, NY 14225.

Mack, E.J., C.W. Rogers and B.J. Wattle, 1983: "An Evaluation of Marine Fog Forecast Concepts and a Preliminary Design for a Marine Obscuration Forecast System." Project SEA FOG IX: Final Report, Calspan Report No. 6866-M-1, June 1983, 252 pp. Calspan Corp., P.O. Box 400, Buffalo, NY 14225.

McGee, T., 1989: Private Communication

Oliver, D.A., W.S. Lewellen amd G.G. Williamson, 1978: "The Interaction Between Turbulent and Radiative Transport in the Development of Fog and Low-Level Stratus, J. Atmos. Sci., 33, pp. 301-316.

Peak, J.E., 1988: "The AESOP 1.0 Expert System." Internal Report, Martin Marietta Data Systems, Monterey, CA 93943-5006, July 1988, 25 pp.

Peak, J.E., 1989: Private Communication

Petterssen, S., 1956: "Weather Analysis and Forecasting, Volume II, Weather and Weather Systems." McGraw-Hill Book Company, Inc. New York, 266 pp.

Rogers, C.W., 1988: "Program Performance Specification for North Atlantic Fog Forecasting." Contractor Report CR 88-12, August 1988. Naval Environmental Prediction Research Facility, Monterey CA 93943-5006, 27 pp.

Rogers, C.W., E.J. Mack, R.J. Pilie, and B.J. Wattle, 1981: "An Investigation of Marine Fog Forecast Concepts." Project Sea Fog Eighth Annual Summary Report, Calspan Report No. 6673-M-1, Contract No. N00019-80-C-0248, January 1981, 97 pp. Calspan Corp., P.O. Box 400, Buffalo, NY 14225.

Taylor, G.I., 1917: "The Formation of Fog and Mist." Quart. J. Roy. Meteor. Soc., 43, 241-268.

Telford, J.W., and S.K. Chai, 1984: "Inversions, and Fog, Stratus and Cumulus Formation in Warm Air Over Cooler Water." Boundary Layer Meteorology, 29, 109-137.

Telford, J.W. and T.S. Keck, 1988; "Atmospheric Structure Generated by Entrainment into Clouds." Atmospheric Research, 22, 191-216

Wattle, B.J., 1987: "Aerosol Characteristics in the Marine Boundary Layer Over the Straits of Gibraltar- June 1986, A Data Volume." Interim Report, Contract No. N00014-85-C-2393, January 1987, 33 pp. Calspan Corp. P.O. Box 400, Buffalo, NY 14225.

DISTRIBUTION LIST

COMMANDER IN CHIEF
U.S. ATLANTIC FLEET
ATTN: FLT METEOROLOGIST
NORFOLK, VA 23511-6001

COMMANDER IN CHIEF
U.S. ATLANTIC FLEET
ATTN: NSAP SCIENCE ADVISOR
NORFOLK, VA 23511-6001

COMMANDER
U.S. NAVAL FORCES, ICELAND
FPO NEW YORK 09571

COMMANDER NAVAL AIR FORCE
U.S. ATLANTIC FLEET
NORFOLK, VA 23511-5188

COMMANDER NAVAL AIR FORCE
U.S. ATLANTIC FLEET
ATTN: NSAP SCIENCE ADVISOR
NORFOLK, VA 23511-5188

COMMANDER
NAVAL SURFACE FORCE
U.S. ATLANTIC FLEET
NORFOLK, VA 23511-6292

COMMANDER
SURFACE WARFARE DEV. GROUP
NAVAMPHIB BASE, LITTLE CREEK
NORFOLK, VA 23521

COMMANDING OFFICER
USS AMERICA (CV-66)
ATTN: MET. OFFICER, OA DIV.
FPO NEW YORK 09531-2790

COMMANDING OFFICER
USS CORAL SEA (CV-43)
ATTN: MET. OFFICE, OA DIV.
FPO NEW YORK 09550-2720

COMMANDING OFFICER
USS D.D. EISENHOWER (CVN-69)
ATTN: MET. OFFICER, OA DIV
FPO NEW YORK 09532-2830

COMMANDING OFFICER
USS FORRESTAL (CV-59)
ATTN: MET. OFFICER, OA DIV.
FPO MIAMI 34080-2730

COMMANDING OFFICER
USS INDEPENDENCE (CV-62)
ATTN: MET. OFFICER, OA DIV
FPO SAN FRANCISCO 96618-2760

COMMANDING OFFICER
USS J.F. KENNEDY (CV-67)
ATTN: MET. OFFICER, OA DIV.
FPO NEW YORK 09538-2800

COMMANDING OFFICER
USS NIMITZ (CVN-68)
ATTN: MET OFFICER, OA DIV.
FPO SEATTLE 98780-2820

COMMANDING OFFICER
USS SARATOGA (CV-60)
ATTN: MET. OFFICER, OA DIV.
FPO MIAMI 34078-2740

COMMANDING OFFICER
USS T. ROOSEVELT (CVN-71)
ATTN: MET. OFFICER, OA DIV.
FPO NEW YORK 09559-2871

COMMANDING OFFICER
USS IOWA (BB-61)
ATTN: MET OFFICER, OA DIV.
FPO NEW YORK 09546-1100

COMMANDING OFFICER
USS WISCONSIN (BB-64)
ATTN: OA DIVISION
FPO NEW YORK 09552-1130

COMMANDING OFFICER
USS MOUNT WHITNEY (LCC-20)
ATTN: MET. OFFICER
FPO NEW YORK 09517-3310

COMMANDING OFFICER
USS GUADALCANAL (LPH-7)
ATTN: MET. OFFICER
FPO NEW YORK 09562-1635

COMMANDING OFFICER
USS GUAM (LPH-9)
ATTN: MET. OFFICER
FPO NEW YORK 09563-1640

COMMANDING OFFICER
USS INCHON (LPH-12)
ATTN: MET. OFFICER
FPO NEW YORK 09529-1655

COMMANDING OFFICER
USS IWO JIMA (LPH-2)
ATTN: MET. OFFICER
FPO NEW YORK 09561-1625

COMMANDING OFFICER
USS NASSAU (LHA-4)
ATTN: MET. OFFICER
FPO NEW YORK 09557-1615

COMMANDING OFFICER
USS SAIPAN (LHA-2)
ATTN: MET. OFFICER
FPO NEW YORK 09549-1605

COMMANDING OFFICER
USS PUGET SOUND (AD-38)
ATTN: METEOROLOGICAL OFFICER
FPO NEW YORK 09544-2520

COMMANDING OFFICER
USS LASALLE (AGF-3)
ATTN: METEOROLOGICAL OFFICER
FPO NEW YORK 09577-3320

COMMANDING GENERAL (G4)
FLEET MARINE FORCE, ATLANTIC
ATTN: NSAP SCIENCE ADVISOR
NORFOLK, VA 23511

OFFICE OF NAVAL RESEARCH
CODE 1122AT, ATMOS SCIENCE
ARLINGTON, VA 22217-5000

OFFICE OF NAVAL RESEARCH
ENV. SCI. PROGRAM, CODE 112
ARLINGTON, VA 22217-5000

OFFICE OF NAVAL RESEARCH
CODE 1122, OCEAN SCI. DIV.
ARLINGTON, VA 22217-5000

OFFICE OF NAVAL RESEARCH
CODE 1122MM, MARINE METEO.
ARLINGTON, VA 22217-5000

COMMANDING OFFICER
NAVAL OCEANOGRAPHIC OFFICE
JCSSC, MS 39522-5001

COMMANDING OFFICER
NAVEASTOCEANCEN
MCADIE BLDG. (U-117), NAS
NORFOLK, VA 23511-5399

NAVAL POSTGRADUATE SCHOOL
METEOROLOGY DEPT.
MONTEREY, CA 93943-5000

COMMANDER
AWS/DNXS
SCOTT AFB, IL 62225

DIRECTOR (6)
DEFENSE TECH. INFORMATION
CENTER, CAMERON STATION
ALEXANDRIA, VA 22314

DIRECTOR
TECHNIQUES DEVELOPMENT LAB
GRAMAX BLDG.
8060 13TH ST.
SILVER SPRING, MD 20910

WOODS HOLE OCEANO. INST.
DOCUMENT LIBRARY LO-206
WOODS HOLE, MA 02543

AMERICAN METEORO. SOCIETY
METEOR. & GEOASTRO. ABSTRACTS
P.O. BOX 1736
WASHINGTON, DC 20013

DIRECTOR, METEO. & OCEANO.
NATIONAL DEFENSE HDQ.
OTTAWA, ONTARIO, KIA OK2
CANADA

MINISTRY OF DEFENCE
NAVY DEPARTMENT
ADMIRALTY RESEARCH LAB
TEDDINGTON, MIDDX ENGLAND

LIBRARY
IRISH METEOROLOGICAL SERVICE
GLASNEVIN HILL
DUBLIN 9, IRELAND

COMMANDING OFFICER
U.S. NAVOCEANCOMFAC
FPO NEW YORK 09571-0926

COMMANDER (2)
NAVAIRSYSCOM
ATTN: LIBRARY (AIR-723D)
WASHINGTON, DC 20361-0001

USAFETAC/TS
SCOTT AFB, IL 62225

DIRECTOR
NATIONAL METEORO. CENTER
NWS, NOAA
WWB W32, RM 204
WASHINGTON, DC 20233

HEAD, ATMOS. SCIENCES DIV.
NATIONAL SCIENCE FOUNDATION
1800 G STREET, NW
WASHINGTON, DC 20550

CHAIRMAN, METEOROLOGY DEPT.
PENNSYLVANIA STATE UNIV.
503 DEIKE BLDG.
UNIVERSITY PARK, PA 16802

WORLD METEOROLOGICAL ORG.
CASE POSTALE #5, CH-1211
GENEVA, SWITZERLAND

DIRECTOR OF NAVAL OCEANO.
& METEOROLOGY
MINISTRY OF DEFENCE
LACON HOUSE, THEOBOLD RD.
LONDON WC 1XBRY, ENGLAND

EUROPEAN CENTRE FOR MEDIUM
RANGE WEATHER FORECASTS
SHINFIELD PARK, READING
BERKSHIRE RG29AX, ENGLAND

COMMANDER
NAVAL OCEANOGRAPHY COMMAND
JCSSC, MS 39529

SUPERINTENDENT
LIBRARY REPORTS
U.S. NAVAL ACADEMY
ANNAPOLIS, MD 21402

COMMANDER
NAVOCEANSYSCEN
DR. J. RICHTER, CODE 54
SAN DIEGO, CA 92152-5000

AFGL/LY
HANSCOM AFB, MA 01731

DIRECTOR
ATLANTIC MARINE CENTER
COAST & GEODETIC SURVEY
439 W. YORK ST.
NORFOLK, VA 23510

SCRIPPS INSTITUTION OF
OCEANOGRAPHY, LIBRARY
DOCUMENTS/REPORTS SECTION
LA JOLLA, CA 92037

THE EXECUTIVE DIRECTOR
AMERICAN METEORO. SOCIETY
45 BEACON ST.
BOSTON, MA 02108

CHAIRMAN, METEOROLOGY DEPT.
MCGILL UNIVERSITY
805 SHERBROOKE ST., W.
MONTREAL, QUEBEC
CANADA H3A 2K6

METEORO. OFFICE LIBRARY
LONDON ROAD
BRACKNELL, BERKSHIRE
RG 12 1SZ, ENGLAND

ICELANDIC MET. OFFICE
BUSTAOAVEGUR 9
105 REYKJAVIK, ICELAND

COMMANDER IN CHIEF FLEET
STAFF METEOROLOGIST &
OCEANOGRAPHY OFFICER
NORTHWOOD, MIDDLESEX HA6 3HP
ENGLAND